A Section 508–conformant HTML version of this article is available at https://doi.org/10.1289/EHP14014.

Estimating Heat-Related Mortality Burden Changes under Type-Specific Green and Blue Space Scenarios in China

Kejia Hu,[1,2] Shiyi Wang,[3*] Fangrong Fei,[4] Jingqiao Fu,[5] Yujie Shen,[1] Feng Chen,[6] Yunquan Zhang,[7] Jian Cheng,[8] Xuchao Yang,[5,9] Jieming Zhong,[4] Yuming Guo,[10] and Jiayu Wu[3]*

[1]Center of Clinical Big Data and Analytics of the Second Affiliated Hospital and School of Public Health, Zhejiang University School of Medicine, Hangzhou, China
[2]Zhejiang Key Laboratory of Intelligent Preventive Medicine, Hangzhou, China
[3]College of Agriculture and Biotechnology, Zhejiang University, Hangzhou, China
[4]Zhejiang Provincial Center for Disease Control and Prevention, Hangzhou, China
[5]Ocean College, Zhejiang University, Zhoushan, China
[6]Zhejiang Institute of Meteorological Sciences, Hangzhou, China
[7]School of Public Health, Wuhan University of Science and Technology, Wuhan, China
[8]Department of Epidemiology and Health Statistics, School of Public Health, Anhui Medical University, Hefei, China
[9]Key Laboratory of Cities Mitigation and Adaptation to Climate Change in Shanghai, China Meteorological Administration, Shanghai, China
[10]Department of Epidemiology and Preventive Medicine and Climate, Air Quality Research Unit, School of Public Health and Preventive Medicine, Monash University, Melbourne, Australia

Background: Green and blue spaces (GBS) are assumed to mitigate heat-induced health risks. However, few studies have explored the impact of type-specific GBS changes on heat-related mortality burden.

Objectives: This study aimed to investigate the effect modifications of different GBS types on heat-related mortality risks, and to estimate the changes in mortality burden in multiple GBS scenarios.

Methods: A case time-series study design was utilized based on the daily data on all-cause mortality and temperatures from 2009 to 2020 in 1,085 subdistricts in China. Mortality count data were obtained from the Zhejiang Center for Disease Control and Prevention. Meteorological data on temperature and relative humidity were acquired from the Zhejiang Meteorological Bureau. GBS exposure was assessed by integrating fine-scale population density, GBS boundary from Baidu and OpenStreetMap, and street-view image data from Baidu. Conditional Poisson regression analyses were conducted with the distributed lag nonlinear model, incorporating modifiers of type-specific GBS exposure. Changes in heat-attributable mortality under different GBS scenarios were also assessed.

Results: Heat-related mortality risks were lower for populations with high exposure (95%) than for those with low exposure (5%) *a*) to overall green spaces, forests, parks, nature reserves, and street greenery, rather than to grasses, farms, and scrubs; and *b*) to overall blue spaces, lakes, and rivers, rather than reservoirs, wetlands, or coasts. Increases of 10%, 20%, and 30% exposure to overall green spaces are expected to avoid heat-related mortality burden by 1.6% [95% empirical confidence interval (eCI): 1.4, 1.9, 3.2% (95% eCI: 2.5, 3.9), and 4.8% (95% eCI: 3.5, 6.2)], respectively, whereas corresponding estimates for overall blue spaces are 5.4% (95% eCI: 4.4, 6.4), 10.8% (95% eCI: 8.5, 13.3), and 16.2% (95% eCI: 12.3, 20.5), respectively. Conversely, a 30% decrease in overall green space exposure and overall blue space exposure will increase the heat-related mortality burden by 4.8% (95% eCI: 4.3, 5.2) and 15.9% (95% eCI: 15.2, 16.7), respectively.

Discussion: Our study revealed differences in the capacity of various GBS types to mitigate heat-related mortality risks. While the protective effects of GBS may be moderate, targeted planning strategies should prioritize their implementation for maximum benefits in mitigating heat-related health risks. The continuous shrinkage of the GBS would render other efforts futile, such as heat–health action plans. https://doi.org/10.1289/EHP14014

Introduction

Increasing heat extremes are considered a primary global environmental challenge of the 21st century, driving numerous negative implications for human health and well-being.[1–3] According to a latest multicountry study, nearly 490,000 deaths per year can be directly or indirectly attributed to excessive natural heat. Asia and China are the most affected continent and country, respectively, accounting for 45% and 15% of heat-related deaths worldwide, respectively.[3] The effects of climate change and urbanization, combined with a rapidly aging population, require innovative strategies to combat heat stress. This need for new strategies is particularly important in cities where urban heat island (UHI) effects are anticipated to cause unprecedented temperatures.[4,5] Heat preparedness and response action plans for individuals and communities (e.g., education, health care infrastructure, and early warning systems) are costly and labor-intensive to implement.[6,7] Nature-based solutions have been increasingly identified as cost-effective and as promising methods for building climate-resilient cities in a long-term efficient and adaptable manner.[8,9]

Green and blue spaces (GBS) are essential nature-based solutions for regulating microclimates through shading and evapotranspiration.[4,10–14] Recent studies have demonstrated that GBS have a protective effect against heat-related mortality risks.[15–17] However, conflicting findings have been reported, suggesting the absence of discernible benefits.[9] The cooling effects of various types of GBS depend on their size, shape, landscape composition, and configuration.[17–19] Furthermore, the impact of GBS on individual outdoor activities and heat exposure during summer may vary by their types.[20,21] Therefore, the heterogeneity in previous findings has been speculated to be associated with the region-

*These authors contributed equally to this paper.
Address correspondence to Jieming Zhong, Zhejiang Provincial Center for Disease Control and Prevention, China. Email: jmzhong@cdc.zj.cn. And, Xuchao Yang, Zhejiang University, China. Email: yangxuchao@zju.edu.cn. And, Yuming Guo, Monash University, Australia. Email: yuming.guo@monash.edu. And, Jiayu Wu, Zhejiang University, China. Email: wujiayula@zju.edu.cn

Supplemental Material is available online (https://doi.org/10.1289/EHP14014).
The authors declare they have nothing to disclose.

Conclusions and opinions are those of the individual authors and do not necessarily reflect the policies or views of EHP Publishing or the National Institute of Environmental Health Sciences.
EHP is a Diamond Open Access journal published with support from the NIEHS, NIH. All content is public domain unless otherwise noted. Contact the corresponding author for permission before any reuse of content. Full licensing information is available online.

Received 18 September 2023; Revised 25 March 2025; Accepted 2 April 2025; Published 22 May 2025.

Note to readers with disabilities: *EHP* strives to ensure that all journal content is accessible to all readers. However, some figures and Supplemental Material published in *EHP* articles may not conform to 508 standards due to the complexity of the information being presented. If you need assistance accessing journal content, please contact ehpsubmissions@niehs.nih.gov. Our staff will work with you to assess and meet your accessibility needs within 3 working days.

specific components of GBS types by directly driving thermal comfort and indirectly influencing human exposure.[20,22] Nevertheless, comparative epidemiological evidence on the combined health effects of different GBS types on potentially increased outdoor exposure time and decreased heat stress are lacking. A limited understanding of the relationships between different types of GBS and the impacts of heat on health hinders the development of effective GBS planning and design strategies to mitigate adverse heat-related health effects.

Although the effect modifications of green or blue spaces on heat-related mortality risks have been examined recently,[15–17] the changes in heat-attributable mortality burden via an increase in GBS exposure have not been assessed extensively. This information can inform the government of the health benefits of maintaining and developing GBS and encourage them to take action. Furthermore, although some cities have been successful in maintaining or expanding their GBS in recent years, others have experienced degradation and destruction of natural vegetation and water bodies due to rapid urban expansion and construction.[23] These changes prompt an inquiry into the impact of potential GBS degradation and destruction on heat-attributable mortality burden, particularly in China, a rapidly urbanizing country.

In this ecological study, exposure indices were developed to reflect residential exposure to overall and type-specific GBS. This goal was achieved by combining fine-scale population distribution data with the GBS maps of nature reserves, forests, parks, farms, scrubs, grasses, coasts, rivers, lakes, wetlands, and reservoirs. Because street greenery has been identified as a significant contributor to cooling,[24] and tree planting is a prevalent method of urban greening, we included street greenery as a type of green space. Exposure to street greenery was assessed using street-view images and a convolutional neural network model because of the scarcity of data sources for measuring street greenery. To investigate the potential impacts of GBS on heat-related health risks, we comprehensively quantified the effect modifications of overall green space, overall blue space, and 12 GBS types on heat–mortality associations in Zhejiang Province, China, between 2009 and 2020. We further estimated the changes in the mortality fraction attributable to heat under different GBS scenarios. This series of calculations reveals the mortality burden that could be prevented through green and blue infrastructure planning strategies or that may be increased due to a decrease in GBS. Our ultimate goal was to provide policymakers and decision-makers with scientific evidence to integrate type-specific GBS planning into climate change adaptation and mitigation measures to build sustainable, climate-resilient, and healthy urban environments.

Methods

Study Area

The study was conducted in Zhejiang Province in China, which had a population of 64.56 million in 2020 and a total area of 105,500 km^2 (Figure 1). Zhejiang is located in the middle of the subtropical zone, and its summer climate is characterized by prolonged high temperatures and humidity. Zhejiang comprises 11 cities, with 90 districts under its jurisdiction, and each district comprises several subdistricts. For this study, we selected a subdistrict as the analysis unit because it is the smallest administrative unit in the death reporting system. We excluded subdistricts whose names or boundaries changed during the study period and thereby their daily mortality was not recorded continuously. Ultimately, 1,085 subdistricts were included in the analysis (Figure S1). The mean population of these subdistricts was 46,386 [standard deviation (SD): 51,349], and the average area was 76.1 (SD:60.5) km^2.

Estimation of Daily Population-Weighted Meteorological Variables

Meteorological data on hourly temperature and relative humidity from 1 January 2009 to 30 June 2020 were acquired from the Zhejiang Meteorological Bureau and were subjected to a thoroughly automated quality-control process to remove random errors. The data were gathered from a highly dense observational network of 4,007 automatic weather stations in the Zhejiang Province and its neighboring provinces (Figure S2). The European Center for Medium Range Weather Forecast (ECMWF) Interim Reanalysis (ERA-Interim), the global atmospheric reanalysis dataset, was used to generate gridded three-dimensional (3D) temperature and relative humidity data at a resolution of 0.75 degrees.[25] Based on meteorological observations, ERA-interim, and a digital elevation model (DEM), the hourly temperature and humidity data were interpolated to 1-km resolution using a method described in Hu et al.[26] Five-fold cross-validation was performed for the predicted daily mean temperature to confirm that the interpolation method yielded reliable predictions with negligible bias [$R^2 = 0.93$; root mean square error (RMSE) $= 0.48$°C].

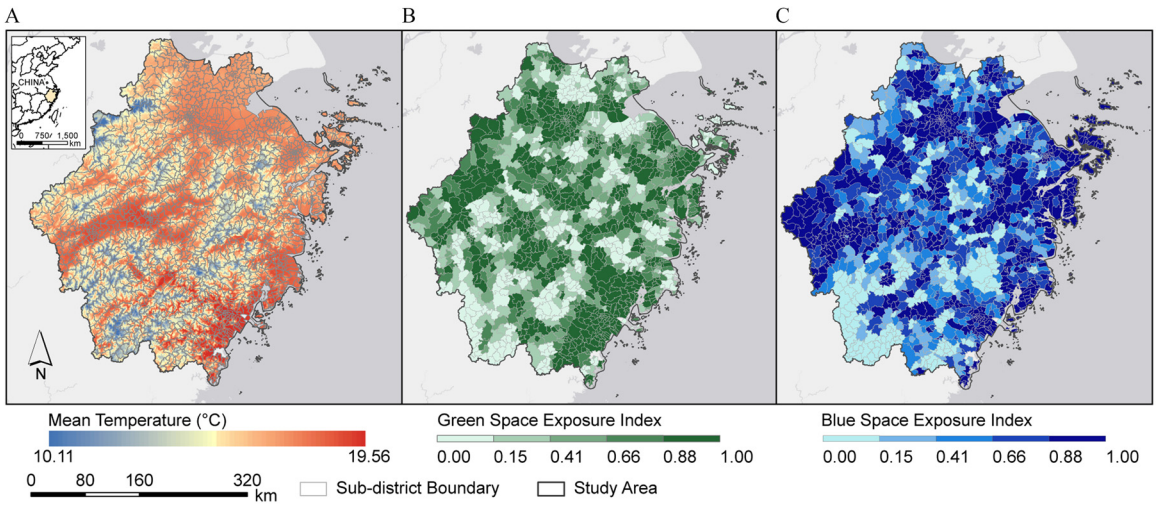

Figure 1. (A) Location of the study area and the averaged daily mean temperature of the area during the study period (2009–2020) of study area. Subdistrict-level overall (B) green and (C) blue space exposure index in Zhejiang Province, China, 2020.

Daily concentrations of particulate matter (PM) with aerodynamic diameter ≤2.5 μm ($PM_{2.5}$) from 1 January 2009 to 30 June 2020 were obtained from the Tracking Air Pollution in China (TAP) dataset (http://tapdata.org.cn). This product was generated using machine learning techniques based on multisource data, including the data from ground-based observations, remote sensing, atmospheric reanalysis, land use, and model simulations. High-quality data for $PM_{2.5}$ with a spatial resolution of 1 km ($R^2 = 0.80–0.88$; RMSE = 13.9–22.1 $\mu g/m^3$) were retrieved from the TAP dataset.[27–29]

The population density in 2010 was estimated at 1-km resolution (Figure S1) using a random forest algorithm based on points-of-interest (POIs), road networks, DEM, and other multisource remote-sensing data, such as those of nighttime light and enhanced vegetation index. The details of these methods have been published by Ye et al.[30] Subsequently, to accurately measure population exposure, the population-weighted averages of the daily 24-h mean temperature, relative humidity, and $PM_{2.5}$ in each subdistrict were calculated.[26]

GBS Exposure Assessments

We developed a green space exposure index to reflect subdistrict-level residents' exposure to overall green spaces (Figure 1) and green spaces based on the type, namely, farms, nature reserves, forests, scrubs, grasses, parks, or street greenery. Polygon green space map data in 2020 for the boundary of farms, nature reserves, scrubs, grasses, and parks were derived from OpenStreetMap (OSM; www.openstreetmap.org), a collaborative project for creating a free global geographic database. OSM provides fairly complete and accurate geographical information of GBS with good quality (Figure S3–S4), in comparison with three other frequently used data sources: Baidu map (map.baidu.com; overlap rate = 99.98%), AMAP (ditu.amap.com; overlap rate = 81.79%), and China Land Use/Cover Dataset (CLUD; https://doi.org/10.5281/zenodo.4417810; overlap rate = 95.18%). Polygon green space map data in 2020 for the boundary of forests were obtained from the Baidu area-of-interest (AOI) dataset, which is the Chinese equivalent of Google Maps. First, buffer zones were created around the input polygons of green spaces (Figure S5) to a specified maximum attraction distance (Table S1; 0.15–10 km) corresponding to different sizes of green spaces.[31–39] The maximum attraction distance represents the maximum range within which the cooling service capacity of green or blue spaces can extend,[31] and it was derived based on the findings from previous studies on the cooling effects of GBS.[32–39] A higher maximum attraction distance was set for larger green space areas. The green space exposure index was generated by calculating the ratio of the number of people residing in the buffer zone of a specific type of green space to the total population of a certain subdistrict.

The green space exposure index of street greenery was assessed using the green view index (GVI), calculated by semantic segmentation of Baidu street-view images. First, the sampling points were selected at 50-m intervals along the urban road network from OpenStreetMap (Figure S6). We chose only the road network in 524 urban subdistricts because the street-view images were scarce in rural subdistricts. Thereafter, 3,314,028 Baidu street-view images were downloaded for the 828,507 sampling points from four angles (0°, 90°, 180°, and 270°) during 2017–2020. The majority (64.6%) of street-view images were captured in summer, when the trees and plants were at their greenest. Other street-view images (35.4%) were captured in spring and autumn, and the images captured in winter were excluded. Although we used a full year's data in statistical analyses to identify the minimum mortality temperature, our main focus was on the effect modifications of GBS on the mortality risks at high temperatures during summer. Therefore, the collection time of street-view images was assumed not to substantially affect our main findings. GVI was derived from street-view images through semantic segmentation using Google's third-generation DeepLab convolutional neural network series, DeepLab V3+.[40] The CityScapes dataset was used to train DeepLab V3+, and the xception71_dpc_cityscapes_trainval model (http://download.tensorflow.org/models/deeplab_cityscapes_xception71_trainvalfine_2018_09_08.tar.gz) was applied. GVI was derived by calculating the mean proportion of vegetation pixels present in the four matched images at each sampling point. The GVI varied between 0 and 1, with a higher value indicating greater street greenery. The mean intersection over union (MIoU), which was often used to measure the accuracy of vegetation pixels being correctly labeled,[41] was estimated to be 87.8%, which indicated a good accuracy of classification results. To determine the green space exposure index for street greenery at the subdistrict level, we first interpolated all point data of GVI values using the kriging method at a spatial resolution of 1 km and calculated the population-weighted GVI in each subdistrict.

The normalized difference vegetation index (NDVI) is a commonly used satellite-derived index for measuring green coverage and is defined as the ratio of the difference between the reflectance in the near-infrared region and red reflectance to the sum of these two measures.[42] Here we used NDVI as a proxy for exposure to overall green space for the sensitivity analysis. All available 2,535 images from Landsat 8 Collection 2 Tier 1 from 2013 to 2020 and 610 images from Landsat 5 Collection 2 Tier 1 from 2009 to 2011 with a resolution of 30 m were downloaded through cloud-based platform of Google Earth Engine (GEE). The annual NDVI composite was generated using the maximum value compositing (MVC) technique, preserving the maximum NDVI value of all available Landsat images for each pixel within each year.[43] The yearly NDVI was selected to account for the temporal variations in green spaces. The mean NDVI values for 2011 and 2013 were used as proxies for the 2012 NDVI value, because there were no Landsat satellite images for 2012. The values of NDVI ranged from −1 to 1, and negative values were excluded before the next calculation. The NDVI data were first resampled to a resolution of 1 km, and the population-weighted NDVI of each subdistrict was calculated.

We also developed a blue space exposure index to assess residents' exposure to overall blue spaces and blue spaces by type, namely lakes, rivers, wetlands, reservoirs, or coast. Polygon data on the inland blue space types of rivers, lakes, wetlands, and reservoirs in 2020 were derived from the Chinese river system and river basin datasets (https://www.rserforum.com/thread/212; Figure S7). The blue space exposure index was generated by calculating the ratio of the number of residents in the buffer zone of a specific type of blue space to the total population of a certain subdistrict. The buffer zones of inland blue spaces were created around the input polygons of blue spaces to a specified maximum attraction distance (1–5 km) corresponding to different types of blue space (Table S2), based on previous research on the cooling effects of blue spaces.[44–53] A buffer zone of the coast was created around the coastline of Zhejiang Province at 5 km.[51]

Mortality and Socioeconomic Data

Daily subdistrict-level mortality count data from 1 January 2009 to 30 June 2020 were obtained from the Zhejiang Center for Disease Control and Prevention. All deaths in Zhejiang must be reported to the surveillance system, which has stringent quality-control measures to ensure data quality.[54] The subdistrict-level percentages of population over 65 y of age, sex ratios, and illiteracy rates in people over 15 y of age were obtained from the 2020 China National Census. District-level per capita disposable

income for 2015 was obtained from the Statistical Yearbook of Zhejiang Province and 11 cities of Zhejiang (e.g., Hangzhou). The socioeconomic status (SES) indicator was measured by adding the *z*-score normalized values of per capita disposable income to the illiteracy rates in population over 15 y of age, as described in previous research.[55]

Statistical Analyses

Time-series daily data on all-cause mortality and ambient mean temperature were collected for 1,085 subdistricts across Zhejiang Province, China, from 1 January 2009 to 30 June 2020. The associations between high temperature and all-cause mortality were explored using a novel case time-series design developed by Gasparrini,[56] modeling a subdistrict-specific series via a fixed-effects conditional quasi-Poisson regression. This design reduces exposure misclassification by allowing exposure and outcomes to be aggregated in a small geographical unit. The regression controlled for the long-term and seasonal trends and the day-of-the-week effect by using strata to match the case and control days within the same subdistrict, year, month, and day of the week. Temperature–mortality associations were modeled using cross-basis functions through distributed lag nonlinear models (DLNMs), which provided a flexible modeling framework to estimate complex nonlinear and delayed effects.[57] A cross-basis function was first defined using a natural cubic spline with two internal nodes at the 33th and 66th percentiles of the mean temperature, and a natural cubic spline for the space of 21 lag days with 3 degrees of freedom. The lag–response association indicated that it was the heat exposure on the same day and the previous 2 d (lag 0–2) that was significantly associated with the increase in mortality risk (Figure S8; Supplemental Excel file S1). Thus, the maximum lag day of high temperatures was then defined as 3 d in cross basis function in DLNM. Minimum mortality temperature (MMT; 18.0°C) was derived from the lowest point of the temperature–mortality association curve (Figure S9; Supplemental Excel file S2),[26] reflecting the most optimum temperature. The effect modifications of GBS on heat-related mortality risk were assessed by adding a linear interaction between the cross-basis function and the green or blue space exposure index.[56,58] Heat temperature was defined using the 95th percentile (P95) of daily population-weighted 24-h temperature, as in previous studies.[59–61] Subsequently, relative risks (RRs) (95th percentile temperature vs. MMT) at low (5%) and high (95%) levels of green or blue space exposure index were predicted. The fifth and 95th percentiles of GBS exposure index were set for defining high and low exposure levels, mainly considering the potential nonnormal distributions of GBS exposure indices and allowing for a comparison across different studies on effect modifiers of GBS.[61–63] To compare RRs at low and high levels of green or blue spaces exposure indices, the ratios of RRs (RRRs) were calculated using the method detailed in Altman and Bland's study,[64] with the *Z*-test as the significance test for the effect modifications of GBS.

For specific types of GBS with a significant effect modification ($p < 0.05$ for *Z*-test) on heat-related mortality, we calculated the attributable fractions (AFs) resulting from temperatures above the MMT in different GBS scenarios. The empirical confidence intervals (95% eCIs) of AFs were obtained by 1,000 Monte Carlo simulations, assuming a multivariate normal distribution for the estimated spline model coefficients.[65] The absolute AF changes and percentages of AF changes were then computed under type-specific green or blue space scenarios: 10%, 20%, or 30% increase, or decrease in the mean value of the green or blue space exposure index.

Next, we conducted sensitivity analyses to verify the robustness of the potential differences in mortality changes at different levels of GBS by *a*) using both time-independent and time-varying annual average NDVI to represent the green space exposure; *b*) reporting RRs at the 10th, 25th, 50th, 75th, and 90th percentiles of the type-specific GBS exposure index; *c*) using half of the original maximum attraction distances and also limited the maximum distances to 5 km, 2 km, and 1 km for green spaces (Table S3) and 2.5 km, 2 km, and 1 km for blue spaces in GBS exposure measurement (Table S4); *d*) additionally adjusting for potential confounders of the percentage of adults over 65 y of age, sex ratio, and SES by adding interactive terms in the regression models, separately; or *e*) additionally adjusting for daily population-weighted 24-h mean $PM_{2.5}$ at 0–1 lag days or for daily population-weighted 24-h mean relative humidity at 0–3 lag days.

In addition, we explored the effect modifications of type-specific GBS on cold-related mortality risk to further investigate the potential underlying mechanism of the influence of GBS on heat-related mortality risks. Cold temperature was defined using the fifth percentile of daily population-weighted 24-h mean temperatures.

All statistical analyses were performed in R (version 4.2.0; R Development Core Team), and the R packages of *dlnm, gnm*, and *MASS* were used. For all statistical tests, the significance level was set at $p < 0.05$ (two-tailed). All maps were produced by ArcGIS 10.5, and the base layers of the maps were obtained by ArcGIS online.

Results

Descriptive Statistics

This study included 2,778,865 all-cause deaths in the 1,085 subdistricts of Zhejiang Province, China, with an average of 241,640 deaths per year. The average daily mean temperature was 16.9°C, ranging between –11.3°C and 36.2°C during the study period (Table 1). The 90th, 95th, and 99th percentiles of the daily mean

Table 1. Descriptive statistics of subdistrict-level ($n = 1,085$) population-weighted daily mean temperature, relative humidity, $PM_{2.5}$, and demographic and socioeconomic variables of percentage of older adults, sex ratio, income, and education in Zhejiang Province, China.

			Percentile					
	Mean ± SD	Min	5	25	50	75	95	Max
Daily mean temperature (°C)	16.89 ± 8.46	−11.32	2.78	9.89	17.78	23.90	29.27	36.23
Daily mean relative humidity (%)	76.56 ± 13.01	14.42	52.85	67.90	77.93	87.04	94.80	100.00
Daily mean $PM_{2.5}$ ($\mu g/m^3$)	34.95 ± 23.69	0.01	9.04	17.92	28.91	45.86	81.23	245.86
People over 65 y of age (%)	13.11 ± 5.83	1.34	4.65	8.93	12.61	16.46	23.42	69.66
Sex ratio (female:male)	1.10 ± 0.09	0.89	0.95	1.04	1.09	1.14	1.26	1.85
Per capita disposable income (RMB Yuan)	31,160 ± 8,931	16,678	17,868	24,051	30,924	38,711	47,052	51,201
Illiteracy rate (%)	4.48 ± 2.43	1.18	1.55	2.67	3.93	4.48	9.34	13.56

Note: $PM_{2.5}$ data was obtained from the Tracking Air Pollution in China (TAP) dataset (http://tapdata.org.cn). Data on percentages of population over 65 y of age, sex ratios, and illiteracy rates in people above 15 y of age were obtained from the 2020 China National Census. Data on per capita disposable income were obtained from the Statistical Yearbook of Zhejiang Province and 11 cities of Zhejiang (e.g., Hangzhou). min, minimum; $PM_{2.5}$, particulate matter with aerodynamic diameter ≤2.5 μm; RMB, renminbi; SD, standard deviation.

temperature were 27.7°C, 29.3°C, and 31.7°C, respectively. The average daily relative humidity was 76.6%. Zhejiang Province, one of China's most mountainous regions, possesses abundant green spaces and water bodies. Consequently, exposure indices for these spaces—representing the proportion of the population within their service buffer zones—are generally high. The mean ± SD values of green space exposure indices were 0.63 (0.40), 0.57 (0.41), 0.21 (0.10), 0.14 (0.28), 0.14 (0.31), 0.02 (0.12), 0.11 (0.26), and 0.02 (0.10) for overall green spaces, forest, street greenery, parks, nature reserves, grasses, farms, and scrubs, respectively. The mean ± SD values of blue space exposure indices were 0.70 (0.35), 0.24 (0.28), 0.28 (0.37), 0.38 (0.39), 0.04 (0.14), and 0.51 (0.49) for overall blue spaces, lakes, rivers, reservoirs, wetlands, and coast, respectively. The distributions of green and blue space exposure indices were provided in Figure S10–S11 and Table S5.

Effect Modifications of GBS

The V-shape curve of temperature and mortality showed that both high and low temperatures increased the risk of mortality (Figure S9). The RR at the 95th percentile of temperature vs. MMT was 1.15 (95% CI: 1.14, 1.16). Significantly lower heat-related mortality risks were found for subdistricts with high levels of green space exposure index for overall green spaces, forests, parks, nature reserves, and street greenery ($p < 0.01$; Figure 2). For instance, for overall green spaces, the RRs (P95 vs. MMT) for specific subdistricts with low and high levels of green space exposure index were 1.18 (95% CI: 1.16, 1.21) and 1.13 (95% CI: 1.12, 1.15), respectively, with the RRR estimated to be 1.05 (95% CI: 1.02, 1.07) (Table S6). However, the effect modification of the green space exposure index of grasses, farms, or scrubs on heat-related mortality risk was not observed.

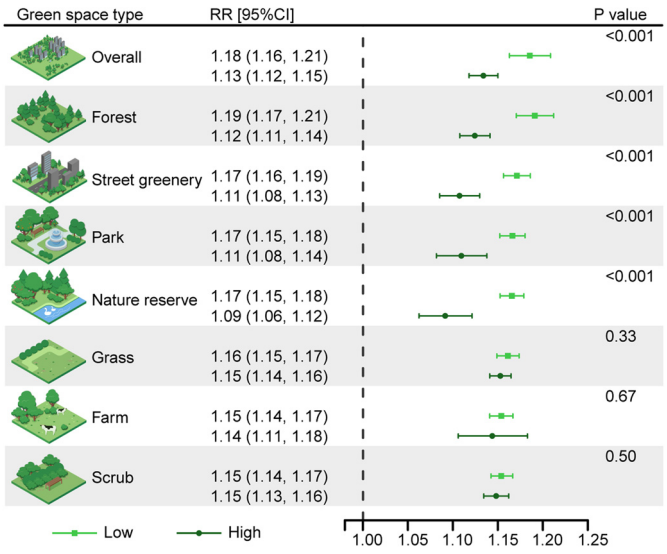

Figure 2. RR and its 95% CI of all-cause mortality at high temperatures (P95, 29.3°C) predicted for a subdistrict with a low (5%, light color) and high (95%, dark color) value of green space exposure index by green space types from case time-series study design in 1,085 subdistricts (524 subdistricts for street greenery) in Zhejiang Province, China, 2009–2020. RRs were derived from fixed-effects conditional quasi-Poisson regressions adjusting for temperature. *p*-Value refers to the significance of the difference between the RRs at the 95th percentile of the temperature (29.3°C) in comparison with MMT (18.0°C) at high (95%) and low (5%) levels of green space exposure index using *Z*-test. Note: CI, confidence interval; P95, 95th percentile of daily mean temperature; MMT, minimum mortality temperature; RR, relative risk.

Differences in heat-related mortality risks were observed for blue space as well, i.e., among subdistricts with low and high exposure levels of overall blue spaces, lakes, and rivers ($p < 0.01$; Figure 3). For example, the RRs (P95 vs. MMT) for specific subdistrict with low and high exposure levels to lakes were 1.18 (95% CI: 1.17, 1.20) and 1.09 (95% CI: 1.06, 1.11), respectively, with an RRR of 1.09 (95% CI: 1.06, 1.12) (Table S7). In contrast, subdistricts with low and high exposure to reservoirs, wetlands, or coasts did not have different heat-related mortality risks.

Attributable Mortality Fractions under Different GBS Scenarios

The mortality fractions attributable to temperatures above the MMT in Zhejiang Province, China, was 2.64% (95% eCI: 2.42, 2.84). The decreases in absolute AFs are expected to be 0.13% (95% eCI: 0.10, 0.15), 0.04% (95% eCI: 0.04, 0.05), 0.16% (95% eCI: 0.14, 0.17), 0.04% (95% eCI: 0.03, 0.04), and 0.08% (95% eCI: 0.07, 0.09) for a 30% increase in the exposure to overall green spaces, nature reserves, forests, parks, and street greenery (Figure 4), respectively; the corresponding percentage decreases in AFs were 4.81% (95% eCI: 3.50, 6.22), 1.60% (95% eCI: 1.29, 1.98), 6.06% (95% eCI: 7.36, 4.86), 1.35% (95% eCI: 1.19, 1.53), and 1.88% (95% eCI: 1.65, 2.13) (Table S10), respectively. Similarly, 10% and 20% increases in the exposure to overall green spaces in all subdistricts are expected to decrease the heat-related AF by 1.60% (95% eCI: 1.35, 1.87) and 3.20% (95% eCI: 2.51, 3.94), respectively, whereas the AF will increase by 1.60% (95% eCI: 1.55, 1.65) and 3.19% (95% eCI: 3.06, 3.29) with 10% and 20% decreases in the exposure to overall green spaces, respectively.

Figure 5 shows a similar pattern that AFs decreased as the exposure to the overall blue spaces, rivers, and lakes increased. Absolute AFs will substantially decrease by 0.14% (95% eCI: 0.13, 0.15), 0.28% (95% eCI: 0.25, 0.32), or 0.42% (95% eCI: 0.39, 0.45), if the exposure to overall blue spaces is increased by 10%, 20%, or 30%, respectively; similarly, the corresponding percentages decreases in AFs will be 5.37% (95% eCI: 4.41, 6.44), 10.77% (95% eCI: 8.52, 13.27), or 16.20% (95% eCI: 12.33,

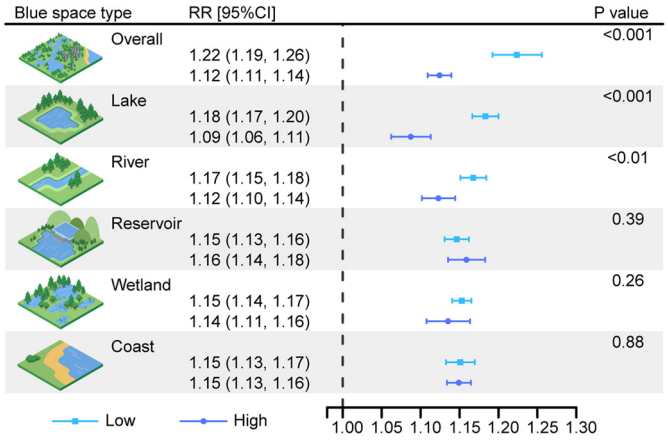

Figure 3. RR and its 95% CI of all-cause mortality at high temperatures (P95, 29.3°C) predicted for a subdistrict with a low (5%, light color) and high (95%, dark color) value of blue space exposure index by blue space types from case time series study design in 1,085 subdistricts in Zhejiang Province, China, 2009–2020. RRs were derived from fixed-effects conditional quasi-Poisson regressions adjusting for temperature. *p*-Value refers to the significance of the difference between the RRs at the 95th percentile of the temperature (29.3°C) in comparison with MMT (18.0°C) at high (95%) and low (5%) levels of blue space exposure index using *Z*-test. Note: CI, confidence interval; P95, 95th percentile of daily mean temperature; MMT, minimum mortality temperature; RR, relative risk.

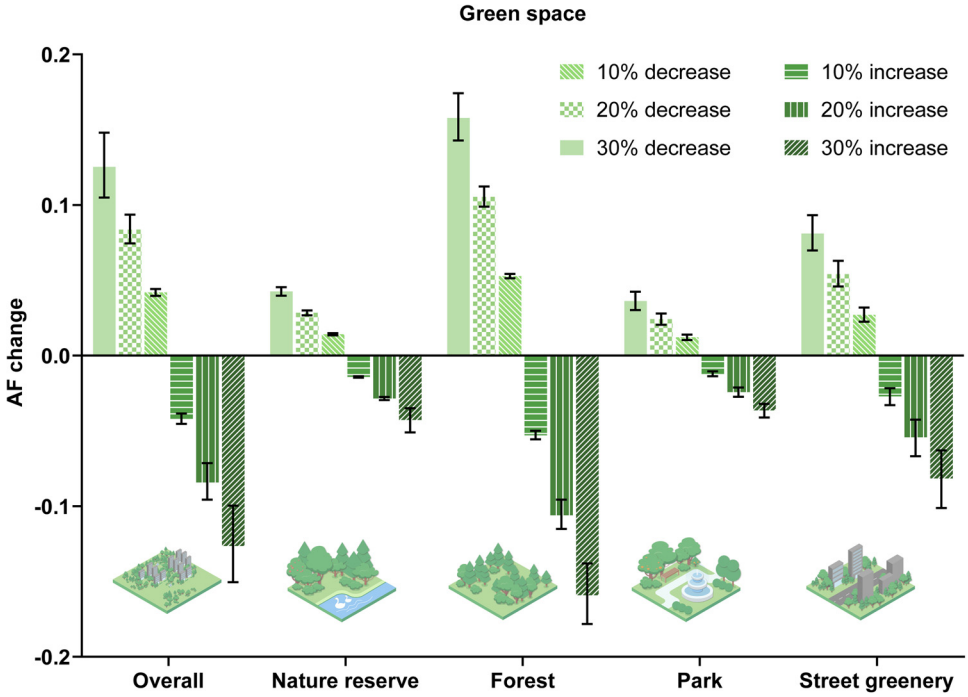

Figure 4. Changes in the absolute value of AF (%) and their 95% eCIs of mortality to high temperature above the MMT under different green space scenarios: 10%, 20%, and 30% increase and decrease of green space exposure index in comparison with the current green space exposure index based on the green space types (i.e., overall green spaces, nature reserves, forests, parks, and street greenery) in 1,085 subdistricts (524 subdistricts for street greenery) in Zhejiang Province, China. Corresponding numeric data are provided in supplementary materials Table S8. The 95% eCIs of AF were obtained by Monte Carlo simulations, assuming a multivariate normal distribution for the estimated spline model coefficients. The baseline GBS exposure indices originated from the year 2020. Note: AF, attributable fraction; eCI, empirical confidence interval; GBS, green and blue spaces; MMT, minimum mortality temperature.

20.49), respectively (Table S11). A 30% increase in the exposure to rivers is expected to decrease the AF by 3.16% (95% eCI: 2.48, 4.00), whereas a 30% increase in the exposure to lakes is expected to decrease the AF by 6.44% (95% eCI: 5.21, 7.94).

Sensitivity Analyses

The heat–mortality associations at high and low levels of the overall green space exposure index and both time-varying and time-independent population-weighted NDVI were consistent, indicating that the green space exposure index can represent greenness exposure as well as NDVI (Figure S12; Supplemental Excel file S3). The analyses reporting RRs at the 10th, 25th, 50th, 75th, and 90th percentiles of the type-specific GBS exposure index (Figure S13–S14; Supplemental Excel file S4–S5) provided valuable insights into the health effects associated with varying levels of GBS exposure and demonstrate a clear trend: decreasing exposure to various types of green and blue space exposure (e.g., forest, street greenery, park, natural reserve, river, and lake) is associated with an increasing risk of heat-related mortality across the exposure spectrum. Sensitivity analyses using changed maximum attraction distances in GBS exposure measurement (Tables S12–S19), or additionally adjusting for the confounders of the percentage of people over 65 y of age, sex ratio, SES, relative humidity, or $PM_{2.5}$ did not alter the effect modifications of specific types of GBS (Figures S15–S24). These sensitivity analyses reinforce the robustness of our main conclusions.

Discussion

To our knowledge, this is the first study to assess heat-attributable mortality burden under multiple type-specific GBS scenarios. We observed that in Zhejiang Province, China, heat-induced premature deaths could be prevented by higher exposure to both green and blue spaces, in accordance with existing evidence from Europe,[66] China,[67] South Korea,[68] and Portugal.[15] Although the cooling effects delivered by various GBS types have been much extensively discussed,[13,20,69,70] it was unclear which type of GBS can preserve the lives of populations in coping with heat. Our findings support that specific GBS types, namely, nature reserves, forests, parks, street greenery, rivers, and lakes, but not grasses, farms, scrubs, reservoirs, wetlands, or coasts, can alleviate the short-term effects of high temperatures on mortality.

Our study highlights that an unevenly distributed GBS may be an important contributor to the spatial heterogeneity in the health impacts of high temperatures. We found that the heat-related mortality risks at extremely high temperatures were 5% (95% CI: 2, 7) and 9% (95% CI: 6, 12) higher in the subdistricts with fewer green and fewer blue spaces, respectively. This estimate is consistent with an earlier literature review that concluded that heat-related mortality risk was ∼5% (95% CI: 0, 11) higher in less vegetated areas.[71] In addition, a multicountry study provided clear evidence that the environmental injustice to retain greenness exposure significantly modified city-level vulnerability to heat, with its relative contribution being greater than that of the proportion of older adults.[72] It also emphasizes the ethical concern that the creation or improvement of GBS in previously dense GBS areas may worsen health inequity, which is especially harmful to vulnerable and disadvantaged groups that often suffer from a lack of high-quality GBS.[2,73] Therefore, targeted efforts to reduce inequalities in GBS access are required to maximize the health benefits of adaptable GBS planning.

Despite growing evidence on the health benefits of green spaces, the mechanisms governing the association between green spaces and heat-related health risks have not been fully elucidated. The protective effects of green space may be related to cooling through direct shading and indirectly through evaporation during

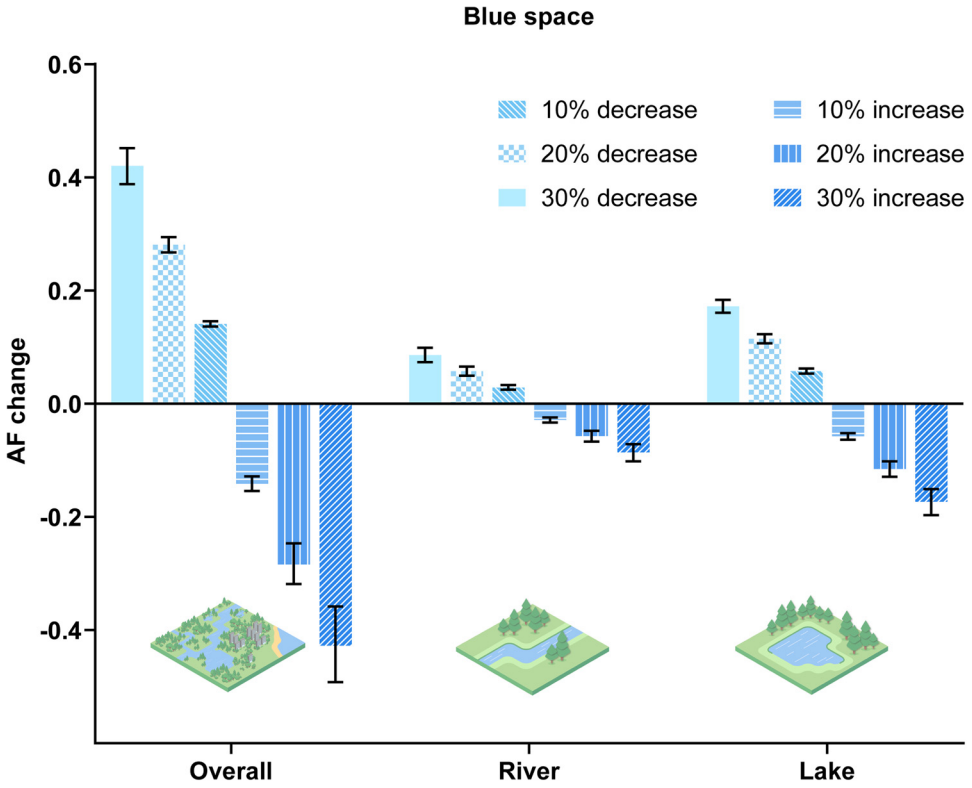

Figure 5. Changes in the absolute value of AF (%) and their 95% eCIs of mortality to high temperature above the MMT under different blue space scenarios: 10%, 20%, and 30% increase and decrease of blue space exposure index in comparison with the current blue space exposure index by blue space types (i.e., overall blue spaces, rivers, and lakes) in 1,085 subdistricts in Zhejiang Province, China. Corresponding numeric data are provided in supplementary materials Table S9. The 95% eCIs of AF were obtained by Monte Carlo simulations, assuming a multivariate normal distribution for the estimated spline model coefficients. The baseline GBS exposure indices originated from the year 2020. Note: AF, attributable fraction; eCI, empirical confidence intervals; GBS, green and blue spaces; MMT, minimum mortality temperature.

the daytime.[74] The absence of an observable effect of green spaces on cold mortality (Table S20) supports this view, because green spaces are more effective at regulating temperatures in summer than in winter.[75,76] The effectiveness of green space cooling is determined by its size, shape, landscape composition, and configuration.[17–19] The size of green spaces has been speculated to be a major factor affecting effect modification. In our analysis, the large green spaces of parks, nature reserves, and forests produced stronger effects than those produced by the small green spaces of grasses, farms, or scrubs. This finding supports previous findings that heat mitigation requires a minimum area of green space to be effective and that a larger green space would achieve greater cooling effect transport into the surrounding environments.[22,77,78] In addition, green spaces have also been linked to positive behaviors such as increased physical activity and social cohesion, which could promote human health and improve people's adaptive capacity to heat stress.[79–81] This pathway may be closely related to street greenery and recreational green spaces such as urban parks.[82] Our findings suggest that green spaces generally have a beneficial effect on heat-related mortality, which could alleviate concerns regarding increased health risks related to potentially enhanced outdoor exposure. In summary, the addition of specific types of green infrastructural networks may aid in achieving the public health goals to address urban heat stress.

Blue spaces have long been considered vital components of adaptation strategies for providing cooling benefits through evaporation.[83] The ability of a blue space to modify thermal comfort is largely determined by its patch area.[17–19] Larger water bodies (e.g., oceans, lakes, and rivers) often absorb more heat radiation than do smaller bodies (e.g., reservoirs and ponds).[17,18] It could explain why the reservoir did not present a protective effect in our analysis. However, we found that higher exposure to the coast did not reduce the risk of heat-related mortality, which challenges the findings in Canada[84] and Portugal[15] but is in agreement with the findings in Hong Kong.[9] Based on the inconsistent results for cold-related mortality risks (Table S21), the potential reasons for this should be further explored. In addition, wetlands were not found to modify the heat–mortality associations. Possible reasons may include only a small proportion of residences covered by the cooling buffer of the wetlands; however, further investigation is required.

The scenario analysis predicted moderate decreases (1.6%–3.2% for overall green space and 5.4%–10.8% for overall blue space) in heat-related mortality burden benefiting from the 10%–20% increases in GBS exposures. Under an ambitious greening scenario with a 30% increase, 4.8% of the total heat-induced mortality was avoided. Although management strategies of developing GBS can only reduce a moderate proportion of heat-related mortality, as estimated by a French study,[66] this approach should nevertheless be prioritized considering the multiple health benefits (e.g., reduced stress and enhanced physical activity) offered by GBS exposure. To maximize the benefits of green space on heat-related health risks, practices such as the protection of nature reserves and forests are needed, and actions to build new or enhance existing parks and street greenery should be taken, for example, to optimize the spatial configuration of urban parks and expand the tree canopy of street greenery.[22,85] Blue space planning decisions for artificial rivers and lakes should be informed by assessing the cooling effectiveness of spaces with different sizes and shapes.[17,18] Furthermore, the increased mortality in

scenarios of decreased GBS exposure emphasizes that policymakers should pay close attention to the health threat of human-made losses to GBSs. For example, the continuous shrinkage of GBS would render other efforts, such as heat–health action plans, futile.

The primary strength of our study is the addition of an epidemiological perspective to the existing literature beyond linking GBS types and their cooling effects to heat-related mortality based on a large sample of nearly 3 million deaths during a relatively long study period. The predominant approach in ecological studies investigating the effects of GBS on health risks is to use area-averaged satellite-derived indices (e.g., NDVI), the coverage of GBS, or the proximity to GBS (e.g., the distance to a water body) to assess green or blue space exposure.[9,21,81] However, this makes it difficult to distinguish between various GBS types; further, such area-level aggregation processes do not consider the spatial distribution of the population and are confronted with the modifiable areal unit problem (MAUP), potentially leading to bias or errors in the exposure measurement.[86] The GBS exposure index developed in our study overcomes the MAUP and exposes it to the effects of type-specific GBS. In addition, a scenario-based analysis is worthwhile for understanding how much of the heat-related mortality burden can be prevented by GBS planning, which could provide scientific evidence for supporting future climate change adaptation and mitigation policies.

Our study had some limitations. First, although we modeled the temperature–mortality associations at a relatively smaller geographical level than those used in previous ecological studies,[68,87,88] owing to private policies, we were unable to obtain information on residential addresses and population movements. Therefore, the relatively large average area of the subdistricts (76 km^2) still introduces a substantial degree of measurement error in individual GBS exposure, because individuals residing within the same subdistrict are assigned the same exposure value despite potential variations in their actual access. Second, although the study considered several demographic and socioeconomic confounders, uncontrolled confounding factors (e.g., noise and the use of air conditioning), owing to the unavailability of appropriate data, may have biased the results.[6,7] Third, in our GBS exposure assessment, the applied maximum attraction distance considered only the size of the GBS; however, the spatial extent of the impact of the GBS may also vary by GBS type. Future studies should use size- and type-specific maximum attraction distances. Fourth, to maximize statistical power, we did not stratify mortality by the cause of death, age, or sex. This approach limited us from exploring the effect modification of GBS types in different age groups, sexes, and specific causes of death.

In summary, this study revealed differences in the capacity of various GBS types to mitigate heat-related mortality risks. The findings can provide evidence-based guidelines for type-specific GBS planning strategies in cities to foster resilience in the face of warming climates. An important consideration is that this study suggests that the benefits of other heat–health action plans can easily be outweighed by the shrinking GBS. Therefore, although the protective effects of GBS may be moderate, targeted planning strategies should prioritize their implementation for maximum benefits in mitigating heat-related health risks.

Acknowledgments

The assistance of Antonio Gasparrini in study design and statistical processes is greatly appreciated.

Contributions of the authors were as follows: K.H.: conceptualization, formal analysis, investigation, software, writing (original draft preparation). S.W.: investigation, software, writing (review and editing). F.F.: data curation, writing (original draft preparation). J.F.: data curation. Y.S.: data curation. F.C.: data curation. Y.Z.: methodology. J.C.: methodology. X.Y.: supervision, funding acquisition, writing (review and editing). J.Z.: supervision, writing (review and editing). Y.G.: supervision, methodology, writing (review and editing). J.W.: supervision, funding acquisition, methodology, writing (review and editing).

The study was supported by the Zhejiang Provincial Natural Science Foundation of China (Y23D050006); the National Natural Science Foundation of China (42001013, 41971019, 32271935); the Key Laboratory of Intelligent Preventive Medicine of Zhejiang Province, China (2020E10004); the Leading Innovative and Entrepreneur Team Introduction Program of Zhejiang (2019R01007); and the Healthy Zhejiang One Million People Cohort (20230085).

References

1. Analitis A, Katsouyanni K, Biggeri A, Baccini M, Forsberg B, Bisanti L, et al. 2008. Effects of cold weather on mortality: results from 15 European cities within the PHEWE project. Am J Epidemiol 168(12):1397–1408, PMID: 18952849, https://doi.org/10.1093/aje/kwn266.
2. Basu R. 2009. High ambient temperature and mortality: a review of epidemiologic studies from 2001 to 2008. Environ Health 8(1):40, PMID: 19758453, https://doi.org/10.1186/1476-069X-8-40.
3. Zhao Q, Guo Y, Ye T, Gasparrini A, Tong S, Overcenco A, et al. 2021. Global, regional, and national burden of mortality associated with non-optimal ambient temperatures from 2000 to 2019: a three-stage modelling study. Lancet Planet Health 5(7):e415–e425, PMID: 34245712, https://doi.org/10.1016/S2542-5196(21)00081-4.
4. Ampatzidis P, Kershaw T. 2020. A review of the impact of blue space on the urban microclimate. Sci Total Environ 730:139068, PMID: 32422454, https://doi.org/10.1016/j.scitotenv.2020.139068.
5. Yang G, Wang Y, Zeng Y, Gao GF, Liang X, Zhou M, et al. 2013. Rapid health transition in China, 1990–2010: findings from the Global Burden of Disease Study 2010. Lancet 381(9882):1987–2015, PMID: 23746901, https://doi.org/10.1016/S0140-6736(13)61097-1.
6. Chen K, Zhou L, Chen X, Ma Z, Liu Y, Huang L, et al. 2016. Urbanization level and vulnerability to heat-related mortality in Jiangsu Province, China. Environ Health Perspect 124(12):1863–1869, PMID: 27152420, https://doi.org/10.1289/EHP204.
7. Curriero FC, Heiner KS, Samet JM, Zeger SL, Strug L, Patz JA. 2002. Temperature and mortality in 11 cities of the eastern United States. Am J Epidemiol 155(1):80–87, PMID: 11772788, https://doi.org/10.1093/aje/155.1.80.
8. Maller C, Townsend M, Pryor A, Brown P, St Leger L. 2006. Healthy nature healthy people: 'contact with nature' as an upstream health promotion intervention for populations. Health Promot Int 21(1):45–54, PMID: 16373379, https://doi.org/10.1093/heapro/dai032.
9. Song J, Lu Y, Zhao Q, Zhang Y, Yang X, Chen Q, et al. 2022. Effect modifications of green space and blue space on heat–mortality association in Hong Kong, 2008–2017. Sci Total Environ 838(pt 2):156127, PMID: 35605868, https://doi.org/10.1016/j.scitotenv.2022.156127.
10. Akbari H, Pomerantz M, Taha H. 2001. Cool surfaces and shade trees to reduce energy use and improve air quality in urban areas. Solar Energy 70(3):295–310, https://doi.org/10.1016/S0038-092X(00)00089-X.
11. Bonan GB. 1997. Effects of land use on the climate of the United States. Climatic Change 37(3):449–486, https://doi.org/10.1023/A:1005305708775.
12. Grimmond CSB, Oke TR. 1991. An evapotranspiration-interception model for urban areas. Water Resour Res 27(7):1739–1755, https://doi.org/10.1029/91WR00557.
13. Gunawardena KR, Wells MJ, Kershaw T. 2017. Utilising green and bluespace to mitigate urban heat island intensity. Sci Total Environ 584–585:1040–1055, PMID: 28161043, https://doi.org/10.1016/j.scitotenv.2017.01.158.
14. Oke TR. 1989. The micrometeorology of the urban forest. Phil Trans R Soc Lond B 324(1223):335–349, https://doi.org/10.1098/rstb.1989.0051.
15. Burkart K, Meier F, Schneider A, Breitner S, Canário P, Alcoforado MJ, et al. 2016. Modification of heat-related mortality in an elderly urban population by vegetation (urban green) and proximity to water (urban blue): evidence from Lisbon, Portugal. Environ Health Perspect 124(7):927–934, PMID: 26566198, https://doi.org/10.1289/ehp.1409529.
16. Murage P, Kovats S, Sarran C, Taylor J, McInnes R, Hajat S. 2020. What individual and neighbourhood-level factors increase the risk of heat-related mortality? A case-crossover study of over 185,000 deaths in London using high-resolution climate datasets. Environ Int 134:105292, PMID: 31726356, https://doi.org/10.1016/j.envint.2019.105292.
17. Theeuwes NE, Solcerová A, Steeneveld GJ. 2013. Modeling the influence of open water surfaces on the summertime temperature and thermal comfort in the city. J Geophys Res Atmos 118(16):8881–8896, https://doi.org/10.1002/jgrd.50704.

18. Sun R, Chen L. 2012. How can urban water bodies be designed for climate adaptation? Landsc Urban Plan 105(1):27–33, https://doi.org/10.1016/j.landurbplan.2011.11.018.
19. Wu C, Li J, Wang C, Song C, Chen Y, Finka M, et al. 2019. Understanding the relationship between urban blue infrastructure and land surface temperature. Sci Total Environ 694:133742, PMID: 31756833, https://doi.org/10.1016/j.scitotenv.2019.133742.
20. McDougall CW, Quilliam RS, Hanley N, Oliver DM. 2020. Freshwater blue space and population health: an emerging research agenda. Sci Total Environ 737:140196, PMID: 32783838, https://doi.org/10.1016/j.scitotenv.2020.140196.
21. Pasanen TP, White MP, Wheeler BW, Garrett JK, Elliott LR. 2019. Neighbourhood blue space, health and wellbeing: the mediating role of different types of physical activity. Environ Int 131:105016, PMID: 31352260, https://doi.org/10.1016/j.envint.2019.105016.
22. Bowler DE, Buyung-Ali L, Knight TM, Pullin AS. 2010. Urban greening to cool towns and cities: a systematic review of the empirical evidence. Landsc Urban Plan 97(3):147–155, https://doi.org/10.1016/j.landurbplan.2010.05.006.
23. Du J, Fu Q, Fang S, Wu J, He P, Quan Z. 2019. Effects of rapid urbanization on vegetation cover in the metropolises of China over the last four decades. Ecol Indic 107:105458, https://doi.org/10.1016/j.ecolind.2019.105458.
24. Shashua-Bar L, Hoffman M. 2000. Vegetation as a climatic component in the design of an urban street. Energy Build 31:221–235, https://doi.org/10.1016/S0378-7788(99)00018-3.
25. Dee DP, Uppala SM, Simmons AJ, Berrisford P, Poli P, Kobayashi S, et al. 2011. The ERA-Interim reanalysis: configuration and performance of the data assimilation system. Q J R Meteorol Soc 137(656):553–597, https://doi.org/10.1002/qj.828.
26. Hu K, Guo Y, Hochrainer-Stigler S, Liu W, See L, Yang X, et al. 2019. Evidence for urban–rural disparity in temperature–mortality relationships in Zhejiang province, China. Environ Health Perspect 127(3):037001, PMID: 30822387, https://doi.org/10.1289/EHP3556.
27. Geng G, Xiao Q, Liu S, Liu X, Cheng J, Zheng Y, et al. 2021. Tracking air pollution in China: near real-time PM2.5 retrievals from multisource data fusion. Environ Sci Technol 55(17):12106–12115, PMID: 34407614, https://doi.org/10.1021/acs.est.1c01863.
28. Xiao Q, Zheng Y, Geng G, Chen C, Huang X, Che H, et al. 2021. Separating emission and meteorological contributions to long-term $PM_{2.5}$ trends over Eastern China during 2000–2018. Atmos Chem Phys 21(12):9475–9496, https://doi.org/10.5194/acp-21-9475-2021.
29. Xiao Q, Geng G, Cheng J, Lian F, Li R, Meng X, et al. 2021. Evaluation of gap-filling approaches in satellite-based daily $PM_{2.5}$ prediction models. Atmos Environ 244:117921, https://doi.org/10.1016/j.atmosenv.2020.117921.
30. Ye T, Zhao N, Yang X, Ouyang Z, Liu X, Chen Q, et al. 2019. Improved population mapping for China using remotely sensed and points-of-interest data within a random forests model. Sci Total Environ 658:936–946, PMID: 30583188, https://doi.org/10.1016/j.scitotenv.2018.12.276.
31. Xing L, Liu Y, Liu X. 2018. Measuring spatial disparity in accessibility with a multi-mode method based on park green spaces classification in Wuhan, China. Appl Geogr 94:251–261, https://doi.org/10.1016/j.apgeog.2018.03.014.
32. Mäkinen K, Tyrväinen L. 2008. Teenage experiences of public green spaces in suburban Helsinki. Urban For Urban Green 7(4):277–289, https://doi.org/10.1016/j.ufug.2008.07.003.
33. Stessens P, Canters F, Huysmans M, Khan AZ. 2020. Urban green space qualities: an integrated approach towards GIS-based assessment reflecting user perception. Land Use Policy 91:104319, https://doi.org/10.1016/j.landusepol.2019.104319.
34. Chen J, Chang Z. 2015. Rethinking urban green space accessibility: evaluating and optimizing public transportation system through social network analysis in megacities. Lands Urban Plan 143:150–159, https://doi.org/10.1016/j.landurbplan.2015.07.007.
35. Schipperijn J, Ekholm O, Stigsdotter U, Toftager M, Bentsen P, Kamper-Jørgensen F, et al. 2010. Factors influencing the use of green space: results from a Danish national representative survey. Landsc Urban Plan 95:130–137. https://doi.org/10.1016/j.landurbplan.2009.12.010.
36. Comber A, Brunsdon C, Green E. 2008. Using a GIS-based network analysis to determine urban greenspace accessibility for different ethnic and religious groups. Landsc Urban Plan 86(1):103–114, https://doi.org/10.1016/j.landurbplan.2008.01.002.
37. Wright Wendel HE, Zarger RK, Mihelcic JR. 2012. Accessibility and usability: green space preferences, perceptions, and barriers in a rapidly urbanizing city in Latin America. Landsc Urban Plan 107(3):272–282, https://doi.org/10.1016/j.landurbplan.2012.06.003.
38. Stessens P, Khan AZ, Huysmans M, Canters F. 2017. Analysing urban green space accessibility and quality: a GIS-based model as spatial decision support for urban ecosystem services in Brussels. Ecosyst Serv 28:328–340, https://doi.org/10.1016/j.ecoser.2017.10.016.
39. Van Herzele A. 2005. *'A Tree on Your Doorstep, A Forest on Your Mind': Greenspace Planning at The Interplay Between Discourse, Physical Conditions, and Practice*. Wageningen, The Netherlands: Wageningen University and Research.
40. Chen LC, Zhu Y, Papandreou G, Schroff F, Adam H. 2018. *Encoder-Decoder with Atrous Separable Convolution for Semantic Image Segmentation*. New York, NY: Springer International Publishing, 833–851.
41. Wu J, Wang B, Ta N, Zhou K, Chai Y. 2020. Does street greenery always promote active travel? Evidence from Beijing. Urban For Urban Green 56:126886, https://doi.org/10.1016/j.ufug.2020.126886.
42. Weier J, Herring D. Measuring Vegetation (NDVI & EVI). https://www.earthobservatory.nasa.gov/features/MeasuringVegetation [accessed 20 December 2022].
43. Holben BN. 1986. Characteristics of maximum-value composite images from temporal AVHRR data. Int J Remote Sensing 7(11):1417–1434, https://doi.org/10.1080/01431168608948945.
44. Elliott LR, White MP, Grellier J, Garrett JK, Cirach M, Wheeler BW, et al. 2020. Research note: residential distance and recreational visits to coastal and inland blue spaces in eighteen countries. Landsc Urban Plan 198:103800, https://doi.org/10.1016/j.landurbplan.2020.103800.
45. Karusisi N, Bean K, Oppert J-M, Pannier B, Chaix B. 2012. Multiple dimensions of residential environments, neighborhood experiences, and jogging behavior in the RECORD study. Prev Med 55(1):50–55, PMID: 22564774, https://doi.org/10.1016/j.ypmed.2012.04.018.
46. Klompmaker JO, Laden F, Browning MHEM, Dominici F, Ogletree SS, Rigolon A, et al. 2022. Associations of parks, greenness, and blue space with cardiovascular and respiratory disease hospitalization in the US Medicare cohort. Environ Pollut 312:120046, PMID: 36049575, https://doi.org/10.1016/j.envpol.2022.120046.
47. McDougall CW, Hanley N, Quilliam RS, Bartie P, Robertson T, Griffiths M, et al. 2021. Neighbourhood blue space and mental health: a nationwide ecological study of antidepressant medication prescribed to older adults. Landsc Urban Plan 214:104132, https://doi.org/10.1016/j.landurbplan.2021.104132.
48. Zhou X, Zhang S, Liu Y, Zhou Q, Wu B, Gao Y, et al. 2022. Impact of urban morphology on the microclimatic regulation of water bodies on waterfront in summer: a case study of Wuhan. Build Environ 226:109720, https://doi.org/10.1016/j.buildenv.2022.109720.
49. Sun R, Chen A, Chen L, Lü Y. 2012. Cooling effects of wetlands in an urban region: the case of Beijing. Ecol Indic 20:57–64, https://doi.org/10.1016/j.ecolind.2012.02.006.
50. White MP, Alcock I, Wheeler BW, Depledge MH. 2013. Coastal proximity, health and well-being: results from a longitudinal panel survey. Health Place 23:97–103, PMID: 23817167, https://doi.org/10.1016/j.healthplace.2013.05.006.
51. Hooyberg A, Roose H, Grellier J, Elliott LR, Lonneville B, White MP, et al. 2020. General health and residential proximity to the coast in Belgium: results from a cross-sectional health survey. Environ Res 184:109225, PMID: 32078817, https://doi.org/10.1016/j.envres.2020.109225.
52. Liu S, Wu X, Lopez AD, Wang L, Cai Y, Page A, et al. 2016. An integrated national mortality surveillance system for death registration and mortality surveillance, China. Bull World Health Organ 94(1):46–57, PMID: 26769996, https://doi.org/10.2471/BLT.15.153148.
53. Huynh Q, Craig W, Janssen I, Pickett W. 2013. Exposure to public natural space as a protective factor for emotional well-being among young people in Canada. BMC Public Health 13(1):407, PMID: 23627738, https://doi.org/10.1186/1471-2458-13-407.
54. Yu Z, Yang G, Zuo S, Jørgensen G, Koga M, Vejre H. 2020. Critical review on the cooling effect of urban blue-green space: a threshold-size perspective. Urban For Urban Green 49:126630, https://doi.org/10.1016/j.ufug.2020.126630.
55. Hu K, Yang X, Zhong J, Fei F, Qi J. 2017. Spatially explicit mapping of heat health risk utilizing environmental and socioeconomic data. Environ Sci Technol 51(3):1498–1507, PMID: 28068073, https://doi.org/10.1021/acs.est.6b04355.
56. Gasparrini A. 2022. A tutorial on the case time series design for small-area analysis. BMC Med Res Methodol 22(1):129, PMID: 35501713, https://doi.org/10.1186/s12874-022-01612-x.
57. Gasparrini A. 2011. Distributed lag linear and non-linear models in R: the package dlnm. J Stat Softw 43(8):1–20, PMID: 22003319.
58. Gasparrini A, Masselot P, Scortichini M, Schneider R, Mistry MN, Sera F, et al. 2022. Small-area assessment of temperature-related mortality risks in England and Wales: a case time series analysis. Lancet Planet Health 6(7):e557–e564, PMID: 35809585, https://doi.org/10.1016/S2542-5196(22)00138-3.
59. Ballester J, Quijal-Zamorano M, Méndez Turrubiates RF, Pegenaute F, Herrmann FR, Robine JM, et al. 2023. Heat-related mortality in Europe during the summer of 2022. Nat Med 29(7):1857–1866, PMID: 37429922, https://doi.org/10.1038/s41591-023-02419-z.
60. Sung TI, Wu PC, Lung SC, Lin CY, Chen MJ, Su HJ. 2013. Relationship between heat index and mortality of 6 major cities in Taiwan. Sci Total Environ 442:275–281, PMID: 23178831, https://doi.org/10.1016/j.scitotenv.2012.09.068.
61. Kephart JL, Sánchez BN, Moore J, Schinasi LH, Bakhtsiyarava M, Ju Y, et al. 2022. City-level impact of extreme temperatures and mortality in Latin America. Nat Med 28(8):1700–1705, PMID: 35760859, https://doi.org/10.1038/s41591-022-01872-6.
62. de Schrijver E, Royé D, Gasparrini A, Franco OH, Vicedo-Cabrera AM. 2023. Exploring vulnerability to heat and cold across urban and rural populations in Switzerland. Environ Res Health 1(2):025003, PMID: 36969952, https://doi.org/10.1088/2752-5309/acab78.

63. Song J, Gasparrini A, Fischer T, Hu K, Lu Y. 2023. Effect modifications of overhead-view and eye-level urban greenery on heat-mortality associations: small-area analyses using case time series design and different greenery measurements. Environ Health Perspect 131(9):097007, PMID: 37728899, https://doi.org/10.1289/EHP12589.
64. Altman DG, Bland JM. 2003. Interaction revisited: the difference between two estimates. BMJ 326(7382):219, PMID: 12543843, https://doi.org/10.1136/bmj.326.7382.219.
65. Vicedo-Cabrera AM, Sera F, Gasparrini A. 2019. Hands-on tutorial on a modeling framework for projections of climate change impacts on health. Epidemiology 30(3):321–329, PMID: 30829832, https://doi.org/10.1097/EDE.0000000000000982.
66. Pascal M, Goria S, Wagner V, Sabastia M, Guillet A, Cordeau E, et al. 2021. Greening is a promising but likely insufficient adaptation strategy to limit the health impacts of extreme heat. Environ Int 151:106441, PMID: 33640693, https://doi.org/10.1016/j.envint.2021.106441.
67. He F, Wei J, Dong Y, Liu C, Zhao K, Peng W, et al. 2022. Associations of ambient temperature with mortality for ischemic and hemorrhagic stroke and the modification effects of greenness in Shandong Province, China. Sci Total Environ 851(pt 1):158046, PMID: 35987239, https://doi.org/10.1016/j.scitotenv.2022.158046.
68. Kim EJ, Kim H. 2017. Effect modification of individual- and regional-scale characteristics on heat wave-related mortality rates between 2009 and 2012 in Seoul, South Korea. Sci Total Environ 595:141–148, PMID: 28384570, https://doi.org/10.1016/j.scitotenv.2017.03.248.
69. Macintyre HL, Heaviside C. 2019. Potential benefits of cool roofs in reducing heat-related mortality during heatwaves in a European city. Environ Int 127:430–441, PMID: 30959308, https://doi.org/10.1016/j.envint.2019.02.065.
70. Peng S-S, Piao S, Zeng Z, Ciais P, Zhou L, Li LZX, et al. 2014. Afforestation in China cools local land surface temperature. Proc Natl Acad Sci USA 111(8):2915–2919, PMID: 24516135, https://doi.org/10.1073/pnas.1315126111.
71. Schinasi LH, Benmarhnia T, De Roos AJ. 2018. Modification of the association between high ambient temperature and health by urban microclimate indicators: a systematic review and meta-analysis. Environ Res 161:168–180, PMID: 29149680, https://doi.org/10.1016/j.envres.2017.11.004.
72. Sera F, Armstrong B, Tobias A, Vicedo-Cabrera AM, Åström C, Bell ML, et al. 2019. How urban characteristics affect vulnerability to heat and cold: a multi-country analysis. Int J Epidemiol 48(4):1101–1112, PMID: 30815699, https://doi.org/10.1093/ije/dyz008.
73. Crouse DL, Pinault L, Balram A, Hystad P, Peters PA, Chen H, et al. 2017. Urban greenness and mortality in Canada's largest cities: a national cohort study. Lancet Planet Health 1(7):e289–e297, PMID: 29851627, https://doi.org/10.1016/S2542-5196(17)30118-3.
74. Alavipanah S, Wegmann M, Qureshi S, Weng Q, Koellner T. 2015. The role of vegetation in mitigating urban land surface temperatures: a case study of Munich, Germany during the warm season. Sustainability 7(4):4689–4706, https://doi.org/10.3390/su7044689.
75. Jim CY, Tsang SW. 2011. Ecological energetics of tropical intensive green roof. Energy Build 43(10):2696–2704, https://doi.org/10.1016/j.enbuild.2011.06.018.
76. Guo F, Schlink U, Wu W, Hu D, Sun J. 2023. Scale-dependent and season-dependent impacts of 2D/3D building morphology on land surface temperature. Sustain Cities Soc 97:104788, https://doi.org/10.1016/j.scs.2023.104788.
77. Chang C-R, Li M-H, Chang S-D. 2007. A preliminary study on the local cool-island intensity of Taipei city parks. Landsc Urban Plan 80(4):386–395, https://doi.org/10.1016/j.landurbplan.2006.09.005.
78. Vaz Monteiro M, Doick KJ, Handley P, Peace A. 2016. The impact of greenspace size on the extent of local nocturnal air temperature cooling in London. Urban For Urban Green 16:160–169, https://doi.org/10.1016/j.ufug.2016.02.008.
79. Liu Y, Wang R, Grekousis G, Liu Y, Yuan Y, Li Z. 2019. Neighbourhood greenness and mental wellbeing in Guangzhou, China: what are the pathways? Landsc Urban Plan 190:103602, https://doi.org/10.1016/j.landurbplan.2019.103602.
80. Markevych I, Schoierer J, Hartig T, Chudnovsky A, Hystad P, Dzhambov AM, et al. 2017. Exploring pathways linking greenspace to health: theoretical and methodological guidance. Environ Res 158:301–317, PMID: 28672128, https://doi.org/10.1016/j.envres.2017.06.028.
81. Rojas-Rueda D, Nieuwenhuijsen MJ, Gascon M, Perez-Leon D, Mudu P. 2019. Green spaces and mortality: a systematic review and meta-analysis of cohort studies. Lancet Planet Health 3(11):e469–e477, PMID: 31777338, https://doi.org/10.1016/S2542-5196(19)30215-3.
82. Lu Y, Sarkar C, Xiao Y. 2018. The effect of street-level greenery on walking behavior: evidence from Hong Kong. Soc Sci Med 208:41–49, PMID: 29758477, https://doi.org/10.1016/j.socscimed.2018.05.022.
83. Lai D, Liu W, Gan T, Liu K, Chen Q. 2019. A review of mitigating strategies to improve the thermal environment and thermal comfort in urban outdoor spaces. Sci Total Environ 661:337–353, PMID: 30677681, https://doi.org/10.1016/j.scitotenv.2019.01.062.
84. Crouse DL, Balram A, Hystad P, Pinault L, van den Bosch M, Chen H, et al. 2018. Associations between living near water and risk of mortality among urban Canadians. Environ Health Perspect 126(7):077008, PMID: 30044232, https://doi.org/10.1289/EHP3397.
85. Son JY, Lane KJ, Lee J-T, Bell ML. 2016. Urban vegetation and heat-related mortality in Seoul, Korea. Environ Res 151:728–733, PMID: 27644031, https://doi.org/10.1016/j.envres.2016.09.001.
86. Wong DWS. 2004. The modifiable areal unit problem (MAUP). In: *WorldMinds: Geographical Perspectives on 100 Problems: Commemorating the 100th Anniversary of the Association of American Geographers 1904–2004.* Janelle DG, Warf B, Hansen K, eds. Dordrecht, Netherlands: Springer Science and Business Media, 571–575.
87. Bakhtsiyarava M, Schinasi LH, Sánchez BN, Dronova I, Kephart JL, Ju Y, et al. 2023. Modification of temperature-related human mortality by area-level socioeconomic and demographic characteristics in Latin American cities. Soc Sci Med 317:115526, PMID: 36476939, https://doi.org/10.1016/j.socscimed.2022.115526.
88. Anderson BG, Bell ML. 2009. Weather-related mortality: how heat, cold, and heat waves affect mortality in the United States. Epidemiology 20(2):205–213, PMID: 19194300, https://doi.org/10.1097/EDE.0b013e318190ee08.